

NASA  
TP  
1307  
c.1

# NASA Technical Paper 1307

LOAN COPY? RETURN TO  
AFWL TECHNICAL LIBRARY  
KIRTLAND AFB, N. M.

0123456789



TECH LIBRARY KAFB, NM

## Parameter Estimation Applied to Nimbus 6 Wide-Angle Longwave Radiation Measurements

Richard N. Green and G. Louis Smith

DECEMBER 1978

NASA



0134410

## NASA Technical Paper 1307

# Parameter Estimation Applied to Nimbus 6 Wide-Angle Longwave Radiation Measurements

Richard N. Green and G. Louis Smith

*Langley Research Center  
Hampton, Virginia*



National Aeronautics  
and Space Administration

**Scientific and Technical  
Information Office**

1978

## SUMMARY

A parameter estimation technique has been used to analyze the August 1975 Nimbus 6 Earth radiation budget (ERB) data to demonstrate the concept of deconvolution. The longwave radiation field at the top of the atmosphere is defined from satellite data by a fifth degree and fifth order spherical harmonic representation. The variations of the major features of the radiation field are defined by analyzing the data separately for each two-day duty cycle. A table of coefficient values for each spherical harmonic representation is given along with global mean, gradients, degree variances, and contour plots. In addition, the entire data set is analyzed to define the monthly average radiation field.

## INTRODUCTION

The importance of measuring and determining the Earth's radiation budget (ERB) on global, zonal, and regional scales has been indicated by previous studies (refs. 1 and 2). Since the atmosphere is driven by radiation, a knowledge of the radiation budget is essential for understanding atmospheric processes (refs. 3 and 4). Much of our understanding of large-scale atmospheric processes was made possible by satellite measurements of Earth's radiation budget and the ensuing analysis.

### Deconvolution by Parameter Estimation

The ERB experiment aboard the Nimbus 6 spacecraft has provided valuable data from its wide field of view (WFOV) radiometers. Each data point is an integral of the irradiance from all points within the field of view of the WFOV sensor, a circular region on the Earth approximately  $60^{\circ}$  in diameter. F. B. House of Drexel University proposed that such data, being a convolution of the flux field at the top of the atmosphere, could be deconvoluted to enhance the resolution. Subsequently, the problem was solved by Smith and Green (refs. 5 to 7). Because of the statistical nature of the problem, a parameter estimation approach to the deconvolution problem was formulated. This technique was simulated for both emitted and reflected radiation (wide and medium field of view). Parameter estimation verified the deconvolution concept and helped to define the propagation of errors (ref. 8). The eigenfunctions of the measurement operator were also shown (ref. 7) to be spherical harmonics for emitted radiation measurements, under certain conditions. Presented in this paper are discussions of the deconvolution estimation concept and results obtained by its application to the August 1975 Earth-emitted radiation data obtained with the WFOV ERB sensor aboard the Nimbus 6 satellite.

The parameter estimation approach to deconvolution is followed in this paper. Basically, the radiation field at the top of the atmosphere is modeled in terms of a linear combination of base functions. The influence coefficients, or shape factors, are then computed. These influence coefficients describe the

influence of model parameters on the radiation measurements at satellite altitude and enable the measurements to be expressed as a linear combination of the model parameters. This system of simultaneous measurement equations is solved by the Gauss-Markoff theorem. The parameter estimation approach is quite general and will accommodate various sensor models, spatially varying directional models for the radiation intensity, and elliptical orbital geometries.

Under certain conditions, the eigenfunctions of the measurement operator are spherical harmonics. If these conditions are met, one can take advantage of this by defining the base functions, which model the radiation field, as spherical harmonics. The two conditions are: the sensor integrates incoming radiation over its field of view, with its directional response a function of nadir angle only; and the directional dependence of exiting radiation at any point at the top of the atmosphere is a function only of the zenith angle of the exiting ray. The first condition is satisfied by the ERB radiometer which is modeled by a perfectly black flat-plate sensor with a cosine nadir-angle response. The second condition states that the directional function is independent of latitude, longitude, and azimuth and is a function of the zenith angle only. That is, one directional function serves to describe the directional dependence of exiting radiation for the entire globe. This is a reasonable assumption for longwave radiation.

Not enough is currently known about the spatial variation of the directional dependence of exiting radiation to model it effectively. Moreover, it has been shown in reference 8 that the gross features of the longwave radiation field are rather insensitive to this assumption. For these reasons, the base functions have been chosen as spherical harmonics. This approach has several advantages. The measurement operator integrates the incoming radiation over the sensor field of view. The influence coefficients are expressed in terms of this integration, which is normally performed by a numerical quadrature formula. This numerical integration requires considerable computational effort and introduces errors into the estimation process. Since spherical harmonics are eigenfunctions of the measurement operator, the problems associated with numerical integration are totally eliminated. The increase in accuracy, due to an exact quadrature formula, and the decrease in computational effort are felt to outweigh the consequences of modeling the directional response for longwave radiation as a function of the zenith angle only. Another advantage is that the radiation field is expressed in terms of spherical harmonics which are convenient for computing other descriptive quantities, such as the spatial spectrum of the radiation field. Thus, the parameter estimation technique is formulated in terms of spherical harmonics which simplify the deconvolution and facilitate its understanding. Since the Nimbus 6 orbit is circular (all measurements at the same altitude) and the measurement errors are modeled as independent random variables, the parameter estimation technique is further simplified.

#### Background

The Nimbus 6 ERB WFOV data for August 1975 have been analyzed by various investigators using different techniques. In the past, the data have been

analyzed on a monthly basis to yield an average radiation field for the month. This procedure, however, gives no information on how much the radiation field varies during the month. A monthly average is descriptive of the data only when the variations during the month are small. In this paper, the temporal variation during the month is investigated by dividing the month into eight periods of four days each and analyzing the data for each period separately to produce a short time history of the Earth emitted radiation field. These results are then combined to obtain the monthly mean radiation field. An analysis of these data, reported by Smith et al. (ref. 9), defined the monthly mean radiation field by a global contour plot and the global mean. The data analysis technique (height rectification) employed a geometric shape factor.<sup>1</sup> The same data were analyzed by Weaver (ref. 10) whose approach used the geometric shape factor. It is worth noting the relationship between parameter estimation and height rectification whereby the radiation field at the top of the atmosphere is computed by multiplying the measurements by a single constant or shape factor. The high order terms are attenuated by the WFOV measurement. Height rectification does not compensate for this attenuation. Parameter estimation, however, compensates for the high order attenuation and should lead to more accurate results. Another analysis of these data, by Green and Smith (ref. 11), defined the monthly mean radiation field by a 12th degree spherical harmonic contour plot. This analysis was based on the parameter estimation technique with the added assumption that the data can be averaged over 5° by 5° areas at the top of the atmosphere. This assumption reduces the computational effort but introduces error by smoothing the data. Green and Smith also present a 15th degree spherical harmonic contour plot in reference 12. This analysis was actually extended to degree 36 to demonstrate the ill-posed nature of the deconvolution problem. Definition of the radiation field to degree 36 by the parameter estimation approach, however, would require the inversion of a prohibitively large matrix. Therefore, the data were averaged over 5° by 5° areas and the radiation field was obtained by approximating the orthogonality of spherical harmonics. This approach is necessary to obtain estimates of the high frequency components of the radiation field, but it is not necessary or desirable for the low frequency components such as the global mean, pole-to-pole gradients, and pole-to-equator gradients.

### Objectives

The purpose of this paper is to demonstrate the parameter estimation technique with the Nimbus 6 ERB data. Since this approach yields the best (minimum variance) unbiased linear estimate of the radiation field within the modeling assumptions, it is felt to give more accurate results than previously reported. The analysis is described in detail and the results are presented in numerical form so that direct comparisons can be made. Previously reported results are inadequate for this purpose.

---

<sup>1</sup>Private communication.

## SYMBOLS

$a_n^m, b_n^m$	complex coefficients of spherical harmonics, $\text{W/m}^2$
B	observation matrix
C	vector of spherical harmonic coefficients, $\text{W/m}^2$
$C_n^m, S_n^m$	real coefficients of spherical harmonics, $\text{W/m}^2$
$d\sigma$	differential surface element
F	directional function for emitted radiation, $\text{sr}^{-1}$
$g(\alpha)$	angular response of sensor
h	satellite altitude above R, km
I	radiant intensity, $(\text{W/m}^2)/\text{sr}$
k	number of measurements
L	measurement operator (see eqs. (7) and (8))
m	measured flux at satellite altitude, $\text{W/m}^2$
M	vector of measured fluxes
N	degree of spherical harmonic expansion
$P_n^m$	associated Legendre polynomial of degree n and order m
Q	radiative flux at top of atmosphere, $\text{W/m}^2$
R	radius of surface approximating top of atmosphere ( $R = R_e + 30$ ), km
$R_e$	radius of Earth (6378.165 km)
RMS	root mean square of measurement residual, km
X	spherical harmonic representation of measured flux at satellite altitude, $\text{W/m}^2$
$Z_n^m$	complex spherical harmonic of degree n and order m
$Z_{cn}^m, Z_{sn}^m$	real spherical harmonics of degree n and order m
$\alpha$	cone angle from satellite nadir to point on surface at top of atmosphere, deg

$\alpha_h$	cone angle from satellite nadir to horizon of surface at top of atmosphere, deg
$\beta$	clock angle from north about satellite nadir to point on surface at top of atmosphere, deg
$\gamma$	Earth central angle between satellite nadir and a point on surface at top of atmosphere, deg
$\delta_n^m$	Kronecker delta
$\epsilon$	vector of measurement residuals, $W/m^2$
$\epsilon_i$	i <sup>th</sup> measurement residual, $W/m^2$
$\zeta$	azimuth angle of exiting ray, deg
$\theta$	colatitude, deg
$\lambda_n$	n <sup>th</sup> eigenvalue of the measurement operator
$\sigma_n^2$	n <sup>th</sup> degree variance (see eq. (22)), $W^2/m^4$
$\phi$	longitude, deg
$\psi$	zenith angle of exiting ray, deg
$\omega$	solid angle, sr

Superscripts:

T	transpose
-1	inverse

Subscript:

s	sensor
---	--------

A circumflex (^) over a symbol denotes an estimate.

## DATA

The data used in this study to define the Earth's longwave radiation field for August 1975 were obtained from the Earth radiation budget (ERB) instrument aboard the Nimbus 6 satellite. A description of the ERB instrument is given in reference 9. The data tapes were supplied by the National Oceanic and Atmospheric Administration.

## Earth Radiation Budget Experiment

The ERB instrument obtained both fixed wide-angle and scanning narrow-angle measurements. The data considered here will be the fixed wide-angle irradiance at satellite altitude. One of the data channels recorded the total Earth irradiance (0.2 to 50  $\mu\text{m}$ ) and another channel recorded the shortwave irradiance (0.2 to 3.8  $\mu\text{m}$ ). The longwave contribution is the difference between these two measurements. The longwave irradiance data were then increased 11 percent as a calibration correction. A discussion of this correction is given in reference 9 and accounts for a discrepancy between the ERB experiment fixed wide-angle and scanning narrow-angle measurements. The ERB instrument operated on a duty cycle of two days on and two days off. Irradiance measurements were taken every 16 seconds. There were eight data periods during the month, but two of these did not have sufficient data to be analyzed separately. Approximately 50 000 measurements were gathered during August 1975, but not all of these data could be used in the analyses.

### Data Edit

The data had to be edited to eliminate measurements which were unacceptable for various reasons. Some of the measurements were degraded by exposure to the Sun. In order for the wide-angle radiometer to view the Earth disk from horizon to horizon, the actual field of view was a few degrees larger than the Earth disk and included a thin annulus of deep space. When the satellite was near sunrise or sunset, the Sun came into view and contaminated the measurements. For this reason, measurements were omitted from the set of data when the Sun zenith at the subsatellite point was between  $111.47^\circ$  and  $123.47^\circ$ . Measurements were also omitted if they were greater than  $280 \text{ W/m}^2$  or less than  $50 \text{ W/m}^2$ . Similarly, a measurement which changed by more than  $10 \text{ W/m}^2$  over a 16-sec time interval was considered unacceptable and was omitted from the data set. Another questionable set of data was obtained on August 16, 1975. Starting at 1000 hours GMT, the measurements gradually decreased in value during a full satellite revolution and then seemed to stabilize at values approximately  $30 \text{ W/m}^2$  lower than expected. This occurred at the end of a data acquisition period. The measurements from the next data period did not exhibit this problem. The reason for this gradual decrease in value is not known. Thus, the measurements starting at 1000 hours GMT and continuing for three satellite revolutions, to the end of the data period, were omitted from the data set. The final edited data set contained 45 942 measurements obtained during August 1975.

During part of the orbit, the ERB radiometers viewed the Earth in darkness where the incident shortwave radiation is negligible. However, the direct irradiation of the sensor at spacecraft sunset caused a thermal transient in the measurements. As the field of view passed into darkness, the shortwave measurements rapidly decreased to about  $9 \text{ W/m}^2$  in the first 2 min and continued to decrease during the remaining 30 min to a lower limit of 1 to  $4 \text{ W/m}^2$ . No attempt was made to correct for this transient in the data.

## ANALYSIS

The edited ERB data were used to estimate the radiation field at the top of the atmosphere. The radiation field was modeled as a linear combination of spherical harmonics and the parameters estimated with a least squares estimator.

### Radiation Model

The top of the Earth-atmospheric system was approximated by a sphere of radius  $R$ . The intensity  $I$  of radiation leaving any point  $E$  on this surface is a function of colatitude  $\theta$ , longitude  $\phi$ , and zenith angle  $\psi$  of the exiting ray. (See fig. 1.) The longwave radiative flux  $Q$  at point  $E$  is given by

$$Q(\theta, \phi) = \int_{\zeta=0}^{\zeta=2\pi} \int_{\psi=0}^{\psi=\frac{\pi}{2}} I(\theta, \phi, \psi) \cos \psi \sin \psi d\psi d\zeta \quad (1)$$

where  $\zeta$  is the azimuth of the exiting ray. The intensity was modeled as

$$I(\theta, \phi, \psi) = \frac{1}{\pi} Q(\theta, \phi) F(\psi) \quad (2)$$

where  $F(\psi)$  is a directional function and is dependent upon only the zenith of the exiting ray. Notice that this function defines the directional characteristics of the exiting radiation at every point on the surface. The strength of the radiation at a given point, however, varies with colatitude and longitude and is defined by  $Q(\theta, \phi)$ . Substituting equation (2) into (1) yields the normalization condition for  $F(\psi)$ , that is,

$$2 \int_{\psi=0}^{\psi=\frac{\pi}{2}} F(\psi) \cos \psi \sin \psi d\psi = 1 \quad (3)$$

If the surface radiation is Lambertian, that is, if radiation leaves the surface with equal intensity in all directions, then  $F(\psi) = 1$ . If this is not true, then the directional characteristics can be defined by a limb darkening function, an example of which is given by

$$F(\psi) = \begin{cases} 1.074 \exp[0.106(1 - \sec \psi)] & (0^\circ \leq \psi < 60^\circ) \\ 1.074 \exp[-0.056 + 0.05(1 - \sec \psi)] & (60^\circ \leq \psi < 90^\circ) \\ 0 & (\psi > 90^\circ) \end{cases} \quad (4)$$

This function results from averaging the family of limb darkening functions in reference 13.

#### Measurement Model

Now consider the radiation sensor at satellite altitude  $h$ , as shown in figure 1. The radiation from the Earth incident on the sensor at a colatitude  $\theta_s$  and a longitude  $\phi_s$  is

$$m(\theta_s, \phi_s) = \int_{FOV} I(\theta, \phi, \psi) g(\alpha) d\omega \quad (5)$$

where  $\omega$  is the solid angle at the satellite subtended by the surface element,  $\alpha$  is the cone angle at the satellite from the local vertical to the surface element, and the integration is over the field of view (FOV) of the sensor. The function  $g(\alpha)$  is the angular response of the sensor to incoming radiation and is modeled as a perfectly black flat-plate sensor, or

$$g(\alpha) = \cos \alpha \quad (6)$$

Substituting (6) and (2) into (5) yields

$$m(\theta_s, \phi_s) = \frac{1}{\pi} \int_{FOV} Q(\theta, \phi) F(\psi) \cos \alpha d\omega$$

or

$$m(\theta_s, \phi_s) = \frac{1}{\pi} \int_{\beta=0}^{\beta=2\pi} \int_{\alpha=0}^{\alpha=\alpha_h} Q(\theta, \phi) F(\psi) \cos \alpha \sin \alpha d\alpha d\beta \quad (7)$$

where  $\alpha_h$  is the cone angle from the satellite nadir to the horizon. It is convenient to express this relationship between the measured radiation  $m(\theta_s, \phi_s)$  and the unknown flux  $Q(\theta, \phi)$  as

$$m(\theta_s, \phi_s) = L[Q(\theta, \phi)] \quad (8)$$

where  $L$  denotes the linear integral measurement operator of equation (7). Smith and Green (ref. 7) have shown that the eigenfunctions of this linear operator are spherical harmonics, that is,

$$L[z_n^m(\theta, \phi)] = \lambda_n z_n^m(\theta_s, \phi_s) \quad (9)$$

where  $z_n^m(\theta_s, \phi_s)$  is a spherical harmonic of order  $m$  and degree  $n$  evaluated at the subsatellite point. The associated eigenvalue  $\lambda_n$  is given by

$$\lambda_n = 2 \int_{\alpha=0}^{\alpha=\alpha_h} P_n^0(\cos \gamma) F(\psi) \cos \alpha \sin \alpha d\alpha \quad (10)$$

where  $P_n^0(\cos \gamma)$  denotes the Legendre polynomial of degree  $n$  as a function of the Earth central angle  $\gamma$ . (See fig. 1.)

#### Deconvolution

Because spherical harmonics are eigenfunctions of the measurement operator, it is convenient to let the flux at the surface be represented by a truncated series of spherical harmonics, that is,

$$Q(\theta, \phi) = \sum_{n=0}^N \sum_{m=-n}^n b_n^m z_n^m(\theta, \phi) \quad (11)$$

Also, let the measurements be represented as

$$m(\theta, \phi) = \sum_{n=0}^N \sum_{m=-n}^n a_n^m z_n^m(\theta, \phi) \quad (12)$$

Substituting equations (11) and (12) into (8) gives

$$\sum_{n=0}^N \sum_{m=-n}^n a_n^m z_n^m(\theta_s, \phi_s) = L \left[ \sum_{n=0}^N \sum_{m=-n}^n b_n^m z_n^m(\theta, \phi) \right]$$

but from equation (9)

$$\sum_{n=0}^N \sum_{m=-n}^n a_n^m z_n^m(\theta_s, \phi_s) = \sum_{n=0}^N \sum_{m=-n}^n \lambda_n b_n^m z_n^m(\theta_s, \phi_s)$$

Equating coefficients of like terms gives

$$a_n^m = \lambda_n b_n^m$$

or

$$b_n^m = \frac{a_n^m}{\lambda_n} \quad (13)$$

Thus, the flux at the surface is

$$Q(\theta, \phi) = \sum_{n=0}^N \sum_{m=-n}^n b_n^m z_n^m(\theta, \phi)$$

or

$$Q(\theta, \phi) = \sum_{n=0}^N \sum_{m=-n}^n \frac{a_n^m}{\lambda_n} z_n^m(\theta, \phi) \quad (14)$$

It is seen that the flux depends on the coefficients of the measurement representation  $a_n^m$  and the eigenvalues of the measurement operator  $\lambda_n$ .

### Spherical Harmonics

For the purposes of this analysis, a real formulation of the spherical harmonics was used. Thus, if  $X(\theta, \phi)$  is a real function over a sphere, then a representation of  $X(\theta, \phi)$  is

$$X(\theta, \phi) = \sum_{n=0}^N \sum_{m=0}^n [C_n^m Z_{cn}^m(\theta, \phi) + S_n^m Z_{sn}^m(\theta, \phi)] \quad (15)$$

where  $Z_n^m(\theta, \phi)$  are spherical harmonics given by

$$Z_{cn}^m(\theta, \phi) = \left[ \frac{(2n+1)(n-m)!}{(n+m)!} \left( 2 - \delta_0^m \right) \right]^{1/2} \cos m\phi P_n^m(\cos \theta) \quad (16a)$$

$$Z_{sn}^m(\theta, \phi) = \left[ \frac{(2n+1)(n-m)!}{(n+m)!} \left( 2 - \delta_0^m \right) \right]^{1/2} \sin m\phi P_n^m(\cos \theta) \quad (16b)$$

and  $P_n^m(\cos \theta)$  are associated Legendre polynomials. These polynomials are defined by the following recursive equation:

$$P_0^0(\cos \theta) = 1$$

$$P_1^0(\cos \theta) = \cos \theta$$

$$P_{n+1}^0(\cos \theta) = \frac{1}{n+1} [(2n+1) \cos \theta P_n^0(\cos \theta) - n P_{n-1}^0(\cos \theta)]$$

( $n = 1, 2, \dots$ )

$$P_m^m(\cos \theta) = (2m-1) \sin \theta P_{m-1}^{m-1}(\cos \theta)$$

$$P_{m+1}^m(\cos \theta) = (2m+1) \cos \theta P_m^m(\cos \theta)$$

$$P_{n+1}^m(\cos \theta) = \frac{(2n+1) \cos \theta P_n^m(\cos \theta) - (n+m) P_{n-1}^m(\cos \theta)}{n-m+1}$$

$$\begin{cases} m = 1, 2, \dots, N \\ n = m+1, m+2, \dots, N-1 \end{cases}$$

It follows that these spherical harmonics are orthogonal according to

$$\int_{\text{Sphere}} z_{cn}^m(\theta, \phi) z_{cj}^i(\theta, \phi) d\sigma = \int_{\text{Sphere}} z_{sn}^m(\theta, \phi) z_{sj}^i(\theta, \phi) d\sigma = 4\pi \delta_n^j \delta_m^i \quad (17a)$$

except for

$$\int_{\text{Sphere}} z_{sn}^0(\theta, \phi) z_{sn}^0(\theta, \phi) d\sigma = 0 \quad (17b)$$

Also,

$$\int_{\text{Sphere}} z_{cn}^m(\theta, \phi) z_{sj}^i(\theta, \phi) d\sigma = 0 \quad (17c)$$

With these definitions, the flux at the surface (eq. (14)) becomes

$$Q(\theta, \phi) = \sum_{n=0}^N \sum_{m=0}^n \frac{1}{\lambda_n} [C_n^m Z_{cn}^m(\theta, \phi) + S_n^m Z_{sn}^m(\theta, \phi)]$$

where  $C_n^m$  and  $S_n^m$  are the coefficients of the measurement representation.

### Estimation of Coefficients

Given a discrete set of measurements, it now remains to determine the coefficients of the measurement representation. These coefficients are estimated with a least squares fit to the measurements. Each discrete measurement  $m(\theta_i, \phi_i)$  is expressed as a linear combination of the coefficients; thus, the  $i$ th measurement is given by

$$m(\theta_i, \phi_i) = \sum_{n=0}^N \sum_{m=0}^n [C_n^m Z_{cn}^m(\theta_i, \phi_i) + S_n^m Z_{sn}^m(\theta_i, \phi_i)] + \epsilon_i \quad (18)$$

where  $\epsilon_i$  is the measurement residual, or the difference between the actual measurement and its representation. This equation and the estimation equations to follow can be greatly simplified by ordering the terms such that the coefficient vector is defined as

$$c \equiv (c_0^0, c_1^0, c_1^1, s_1^1, c_2^0, c_2^1, s_2^1, \dots, s_N^N)^T \quad (19)$$

which consists of  $(N + 1)^2$  terms. Note that  $s_n^0$  is not contained in the ordering. From equation (16b), it can be seen that the spherical harmonic  $Z_{sn}^m(\theta, \phi) = 0$  when  $m = 0$ . Hence, its coefficient  $s_n^0$  is meaningless. Also define a measurement vector as

$$M \equiv [m(\theta_1, \phi_1), m(\theta_2, \phi_2), \dots, m(\theta_k, \phi_k)]^T$$

a residual vector as

$$\epsilon \equiv (\epsilon_1, \epsilon_2, \dots, \epsilon_k)^T$$

and an observation matrix as

$$B \equiv \begin{bmatrix} z_{c0}^0(\theta_1, \phi_1) & z_{cl}^0(\theta_1, \phi_1) & \dots & z_{SN}^N(\theta_1, \phi_1) \\ z_{c0}^0(\theta_2, \phi_2) & z_{cl}^0(\theta_2, \phi_2) & \dots & z_{SN}^N(\theta_2, \phi_2) \\ \vdots & \vdots & & \vdots \\ \vdots & \vdots & & \vdots \\ z_{c0}^0(\theta_k, \phi_k) & z_{cl}^0(\theta_k, \phi_k) & \dots & z_{SN}^N(\theta_k, \phi_k) \end{bmatrix}$$

where  $k$  is the number of measurements. The entire set of measurements given by equation (18) is now conveniently expressed in matrix notation by

$$M = BC + \epsilon \quad (20)$$

This is an overdetermined system of simultaneous equations. The solution that minimizes the sum of squares of the residuals  $\epsilon^T \epsilon$  is the least squares solution and is given by (ref. 14)

$$\hat{C} = (B^T B)^{-1} B^T M \quad (21)$$

## RESULTS

The ERB data were analyzed to demonstrate and evaluate the concept of parameter estimation and to define the variation of the longwave radiation field during the month of August 1975. The spatial variation is given by the spherical harmonic functions in colatitude and longitude. The temporal variation was obtained by analyzing the data separately for two day periods. This is a natural division of time since the ERB instrument operated on a duty cycle of two days on and two days off. During the month of August 1975, there were eight duty cycles, two of which had an insufficient number of

measurements to be analyzed separately. Thus, the data were analyzed separately for six duty cycles of two days each, resulting in a short time history of Earth's longwave radiation. In addition, the entire data set for all periods was combined and analyzed to determine a monthly average radiation field.

#### Degree Variance

The data obtained during the first duty cycle (August 2-4) were analyzed, and the radiation field at the surface was defined by a 12th degree and 12th order spherical harmonic expansion where the coefficients were least square estimates (eq. (21)). These coefficients define the spatial spectrum of the radiation field in terms of the degree variance.

The degree variance is defined as the average value of the solution squared for a given degree. If  $X(\theta, \phi)$  is a spherical harmonic representation (eq. (15)), the degree variance is given by

$$\sigma_n^2 = \frac{\int_{\text{Sphere}} X_n^2(\theta, \phi) d\sigma}{\int_{\text{Sphere}} d\sigma} \quad (22)$$

where

$$X_n(\theta, \phi) \equiv \sum_{m=0}^n \left[ C_n^m Z_{cn}^m(\theta, \phi) + S_n^m Z_{sn}^m(\theta, \phi) \right] \quad (23)$$

Substitution of equation (23) into equation (22) along with the orthogonality conditions (eq. (17)) yields

$$\sigma_n^2 = \sum_{m=0}^n \left[ (C_n^m)^2 + (S_n^m)^2 \right]$$

where  $S_n^0$  is defined as zero. The square root of degree variance is called degree dispersion (denoted by  $\sigma_n$ ) and is often used to denote the variation. The degree variance for all  $n$  is analogous to the amplitude spectrum in ordinary harmonic analysis and gives an indication of the power in each frequency. The degree variance for the first duty cycle is shown in figure 2 at both satellite altitude and at the surface. The relationship between the two degree variances follows from equation (13) and is given by

$$\sigma_n^2(\text{surface}) = \frac{\sigma_n^2(\text{altitude})}{\lambda_n^2}$$

where  $\lambda_n$  are the eigenvalues defined by equation (10). Eigenvalues are presented in table I for a Lambertian directional model and for the limb darkening model defined by equation (4). The sequence of eigenvalues is monotonically decreasing and results from the smoothing effect of the measurement operator. Since the amplitude of the high frequency components of the radiation field are reduced by the measurement operator, the inverse process must amplify these components. This can be seen by the divergence in the two degree variances as the degree number increases. Representing the radiation field by increasingly higher degree spherical harmonics will eventually lead to a meaningless representation at the surface due to this divergence. Variations of the radiation field and errors in the measurement produce high frequency components at satellite altitude which are greatly amplified when converted to the surface by the factor  $1/\lambda_n$ . Thus, there is some degree beyond which variability effects and measurement errors dominate. The representation for the first duty cycle, however, seems to be well behaved at least to degree five. Therefore, the radiation field for this study was modeled by a fifth degree and fifth order expansion in spherical harmonics.

#### Estimated Coefficients

The coefficients of the radiation field at satellite altitude are presented in table II for the first six duty cycles in August. Each radiation field is represented by the 36 coefficients of the spherical harmonic expansion. The ordering corresponds to the scheme defined in equation (19). The last column is the monthly average radiation field and covers the period August 2 through August 31. The data set for this radiation field contained 45 942 measurements and incorporated all of the measurements from each of the six duty cycles plus 1978 measurements from the eighth duty cycle. This duty cycle contained good data for about three orbital revolutions which are beneficial to the monthly average but not sufficient to be analyzed separately. The seventh duty cycle contained no data. Also presented in table II is the RMS residual between the measurement and the spherical harmonic representation, that is,

$$\text{RMS} = \left\{ \frac{1}{k} \sum_{i=1}^k [m(\theta_i, \phi_i) - x(\theta_i, \phi_i)]^2 \right\}^{1/2}$$

where  $k$  is the number of measurements. According to equations (18) and (20), the RMS is expressed in matrix notation as

$$\text{RMS} = \left[ \frac{1}{k} \epsilon^T \epsilon \right]^{1/2} = \left[ \frac{1}{k} (\mathbf{M} - \hat{\mathbf{B}}\hat{\mathbf{C}})^T (\mathbf{M} - \hat{\mathbf{B}}\hat{\mathbf{C}}) \right]^{1/2}$$

Expanding this expression and incorporating equation (21), yields

$$\text{RMS}^2 = \frac{1}{k} [\mathbf{M}^T \mathbf{M} - \hat{\mathbf{C}}^T \hat{\mathbf{B}}^T \mathbf{M}]$$

The RMS is a measure of the amount of total variation  $\mathbf{M}^T \mathbf{M}$  that has not been accounted for by the spherical harmonic representation. It is, therefore, an indication of how well the measurements are represented by  $X(\theta, \phi)$ .

The spherical harmonic representation  $X(\theta, \phi)$  of the measurements at satellite altitude is deconvoluted to the surface by dividing by the eigenvalues of the measurement operator (eq. (13)). This transformation is based on the assumed directional function of the radiation at the surface. The radiation field at the surface for Lambertian radiation is presented in table III, and the degree dispersions are presented in table IV. Some of these coefficients have obvious physical meanings. For example, the global mean flux is given by

$$Q_{\text{globe}} = \frac{\int \limits_{\text{Sphere}} Q(\theta, \phi) d\sigma}{\int \limits_{\text{Sphere}} d\sigma}$$

$$= \frac{1}{4\pi} \int \limits_{\text{Sphere}} \sum_{n=0}^N \sum_{m=0}^n [c_n^m z_{cn}^m(\theta, \phi) + s_n^m z_{sn}^m(\theta, \phi)] d\sigma$$

$$= c_0^0$$

All spherical harmonics integrate to zero over the surface except  $Z_{c0}^0(\theta, \phi) = 1$  which integrates to  $4\pi$ . Thus, the first coefficient  $C_0^0$  is the global mean flux at the surface. In addition, the coefficient of the first zonal harmonic  $C_1^0$  is a measure of the pole-to-pole gradient, and the coefficient of the second zonal harmonic  $C_2^0$  is a measure of the equator-to-pole gradient.

### Interpretation of Coefficients

The radiation field for each duty cycle is depicted by a contour plot in figures 3 to 8, and the monthly average radiation field is depicted in figure 9. These representations should not be interpreted as final since they are only fifth degree representations of the radiation field. The data should support a higher degree representation (fig. 2). Nevertheless, a fifth degree representation is sufficient to demonstrate the parameter estimation technique and define the variation of the major features during one month. From the contour plots, it can be seen that the positions of the major highs and lows are rather stable during the month. For this reason, the monthly average plot (fig. 9) is representative of the major features of the radiation field throughout the month. It can also be seen from the contour plots and from the table of coefficients that the radiation fields are zonal in character. This can also be seen by computing the present contribution of the zonal coefficient to the degree variance, that is,  $\left[ \left( C_n^0 \right)^2 / \sigma_n^2 \right] 100\%$ . For the monthly average radiation field, the percentages for increasing degree numbers are as follows: 100, 85, 90, 76, 70, and 17. For degree zero, the entire degree variance is composed of the zonal contribution. The zonal component is also the dominant influence for degrees one to four. Degree five shows more of a balance between the zonal and nonzonal terms. Since the degree variance generally decreases with increasing degree (at least through degree five for this case), the conclusion is reached that the radiation fields are predominately zonal in character.

Insight into the nature of the radiation fields can be obtained by ordering the 36 coefficients according to their importance. This is accomplished by computing the increase in the RMS value when a specific term is omitted, that is, the importance of a term is equated to the increase in the RMS when a 35 coefficient representation is determined. This procedure revealed that the five most important coefficients for the first duty cycle were the first five zonal harmonic coefficients. The 6 zonal harmonic coefficient numbered 10th in importance. Generally, a size ordering of the coefficients follows closely the importance ordering of the coefficients. If the position of the measurements were such that the  $B^T B$  matrix in equation (21) was diagonal, then the two orderings would be identical. This is not true for the Nimbus 6 data since the measurement positions correspond to satellite positions. Nevertheless, for the

data under consideration, the two orderings differed in the first 10 positions only by a rearrangement of the 7th, 8th, and 9th terms.

An alternative to using a complete set of spherical harmonics (i.e., using all the terms in the sequence of eq. (19) for a given  $N$ ) is to use a selected set of harmonics. A subset of the most important harmonics would be appropriate. Consider the first duty cycle. Elimination of all terms except the global mean

flux  $C_0^0$  corresponds to a one term representation with an RMS value of 29.916.

The total variation is defined as the square of this quantity. From table II the RMS value for a 36 term representation is 9.564. Thus, a 36 term solution

accounts for  $\left[ \frac{(29.916)^2 - (9.564)^2}{(29.916)^2} \right] 100\% = 90\%$  of the total variation. Likewise,

a solution based on the 20 most important terms accounts for 88 percent of the total variation and a 10 term solution accounts for 84 percent. Hence, the 10 most important terms account for 84 percent of the total variation, the next 26 terms in importance account for 6 percent, and the 16 least important terms account for only 2 percent.

#### Importance of Directional Model

When the radiation field at satellite altitude is deconvoluted to the surface by equation (13), a directional model must be defined through the eigenvalues. Sets of eigenvalues are presented in table I for a Lambertian model and a limb darkening directional model. The surface radiation fields in table III are based on the Lambertian model. The difference in the surface radiation field resulting from the two different directional models is very small especially for the low frequency terms. The global mean is defined

by the constant term given by  $C_0^0(\text{surface}) = \frac{1}{\lambda_0} C_0^0(\text{altitude})$ . But,  $\lambda_0$  is the

same for both directional models and, in fact, is the same for any directional model defined by the normalizing condition (eq. (3)). Thus, the global mean at the surface is not a function of the directional model. For a fifth degree representation, only the first six eigenvalues are needed. These eigenvalues for the two models differ only slightly. Moreover, most of the power is in the lower frequencies. Hence, the fifth degree representation is not a strong function of the directional models.

#### Time History of Coefficients

A short history of the most important coefficients is presented in figure 10. The change in the global mean estimate  $C_0^0$  from its least value to its largest value is only  $2.0 \text{ W/m}^2$ . Its greatest departure from the monthly mean is  $1.3 \text{ W/m}^2$ . It is seen that the time variations in the other coefficients

are also small. Because they are so small, it is not clear whether they are due to real fluctuations of the atmosphere, sampling variations, or some other cause.

#### CONCLUDING REMARKS

The Nimbus 6 Earth radiation budget data for the month of August 1975 has been analyzed by the parameter estimation technique to define the variation of the longwave radiation field at the top of the atmosphere. Since the eigenfunctions of the measurement operator are spherical harmonics, they provided a convenient representation of the radiation field. Moreover, the coefficient of the first zonal harmonic is the global mean flux, while the coefficients of the second and third zonal harmonics are measures of the pole-to-pole gradient and the equator-to-pole gradient, respectively. It was shown that the zonal harmonics are the most important terms in the representation of the radiation field; that is, the radiation field at the top of the atmosphere is characterized by axial symmetry.

The radiation field was represented as a fifth degree and fifth order expansion in spherical harmonics. Atmospheric variations and random measurement errors cause the representation to diverge in the high frequency components. The degree variance, however, showed that the solution was well behaved through degree five which corresponds to representing the solution in terms of 36 coefficients. Even though a higher degree representation can be supported by the data, a fifth degree solution is sufficient to demonstrate the parameter estimation technique and define the variation of the major features during the month. If the coefficients are ordered according to their importance in reducing the root mean square of the measurement residual, the radiation field can be expressed in terms of a subset of those coefficients. When all 36 coefficients are used, they account for 90 percent of the total variation. A representation based on the 20 most important coefficients accounts for 88 percent of the total variation, and a 10 coefficient representation accounts for 84 percent. Thus, the 10 most important coefficients account for 84 percent of the total variation, the next 26 coefficients in importance account for 6 percent, and the 16 least important coefficients account for only 2 percent.

The data were analyzed for two-day periods of time resulting in a short time history. The coefficients corresponding to the low frequency zonal harmonics are fairly constant with time. For example, the change in the global mean estimate from its least value to its largest value was only  $2.0 \text{ W/m}^2$ , or less than 1 percent. Its greatest departure from the monthly mean was  $1.3 \text{ W/m}^2$ . Because these changes are small, it is not clear whether they are due to real fluctuations of the atmosphere, sampling variations, or some other cause.

When the radiation field at satellite altitude is deconvoluted to the top of the atmosphere, the directional characteristics of the radiation field must be defined and are expressed through the eigenvalues of the measurement operator. Examination of these eigenvalues shows that the representation to fifth

degree is not strongly affected by these characteristics. In fact, the global mean is seen to be independent of the directional model.

Langley Research Center  
National Aeronautics and Space Administration  
Hampton, VA 23665  
September 19, 1978

## REFERENCES

1. Remote Measurement of Pollution. NASA SP-285, 1971.
2. Inadvertent Climate Modification: Report of the Study of Man's Impact on Climate (SMIC). MIT Press, c.1971.
3. Kellogg, William W.: The Earth's Climate as Seen From Space. *Acta Astronaut.*, vol. 1, no. 1/2, Jan./Feb. 1974, pp. 81-91.
4. Understanding Climatic Change - A Program for Action. Natl. Acad. Sci.-Nat. Res. Counc., 1975.
5. Smith, G. Louis; and Green, Richard N.: A Technique for Analysis of Low Resolution Measurements of Earth Radiation Budget. Second Conference on Atmospheric Radiation, American Meteorol. Soc., Oct. 1975, pp. 111-114.
6. Smith, G. Louis; Green, Richard N.; and Campbell, G. G.: A Statistical Interpretation Technique for Wide Angle Radiometer Measurements of Earth Energy Budget. Fourth Conference on Probability and Statistics in Atmospheric Science, American Meteorol. Soc., Nov. 1975, pp. 171-176.
7. Smith, G. Louis; and Green, Richard N.: Theoretical Analysis of Wide Field of View Radiometer Measurements of Earth Energy Budget. NASA paper presented at Fifth Annual Remote Sensing of Earth Resources Conference (Tullahoma, Tenn.), Mar. 29-31, 1976.
8. Green, Richard N.: Simulation Studies of Wide and Medium Field of View Earth Radiation Data Analysis. NASA TP-1182, 1978.
9. Smith, W. L.; Hickey, J.; Howell, H. B.; Jacobowitz, H.: Hilleary, D. T.; and Drummond, A. J.: Nimbus-6 Earth Radiation Budget Experiment. *Appl. Opt.*, vol. 16, no. 2, Feb. 1977, pp. 306-318.
10. Weaver, William L; and Green, Richard N.: Analysis of Simulated Measurements of Earth Emitted Radiation Using Geometric Shape Factors and Some Results From Analysis of ESSA 7 and Nimbus 6 Data. NASA paper presented at Third Conference on Atmospheric Radiation (Davis, Calif.), June 28-30, 1978.
11. Green, R. N.; and Smith, G. L.: Deconvolution of Earth Radiation Budget Data. Third National Aeronautics and Space Administration Weather and Climate Program Science Review, NASA CP-2029, 1977, pp. 299-303.
12. Green, R. N.; and Smith, G. L.: Deconvolution Estimation Theory Applied to Nimbus 6 ERB Data. Third Conference on Atmospheric Radiation, American Meteorol. Soc., c.1978, pp. 376-379.

13. Raschke, Ehrhard; Vonder Haar, Thomas H.; Pasternak, Musa; and Bandeen, William R.: The Radiation Balance of the Earth-Atmosphere System From Nimbus 3 Radiation Measurements. NASA TN D-7249, 1973.
14. Liebelt, Paul B.: An Introduction to Optimal Estimation. Addison-Wesley Pub. Co., Inc., c.1967.

TABLE I.- EIGENVALUES OF MEASUREMENT OPERATOR

$$\left[ \begin{array}{l} R = R_e + 30.000 \text{ km} = 6408.165 \text{ km;} \\ h = 1100 \text{ km} - 30 \text{ km} = 1070 \text{ km} \end{array} \right]$$

n	$\lambda_n$ for -	
	Lambertian model	Limb darkening model
0	0.7343	0.7343
1	.7217	.7232
2	.6975	.7014
3	.6632	.6704
4	.6208	.6317
5	.5726	.5873
6	.5214	.5393
7	.4693	.4899
8	.4185	.4408
9	.3707	.3936
10	.3267	.3494
11	.2874	.3091
12	.2526	.2728

TABLE II.- COEFFICIENTS OF SPHERICAL HARMONIC REPRESENTATION AT SATELLITE ALTITUDE

n	m	Coefficient	Coefficients for duty cycle -						
			1	2	3	4	5	Monthly average	
0	0	C	173.024	172.430	172.319	173.212	173.826	173.106	172.860
1	0	C	8.911	8.058	9.060	8.550	8.586	7.696	8.535
	1	C	3.624	3.662	2.598	2.663	2.828	1.766	2.689
		S	-2.739	-1.768	-2.759	-3.197	-1.653	-1.307	-2.358
2	0	C	-15.906	-16.088	-14.980	-16.782	-16.651	-16.627	-16.074
	1	C	2.229	4.066	3.904	2.042	2.581	2.602	2.777
2		S	-.731	-1.670	-1.763	-.800	-.832	-1.518	-1.203
	2	C	2.815	4.044	3.696	3.693	2.896	3.589	3.477
		S	3.606	2.715	3.842	1.913	2.162	1.223	2.619
3	0	C	8.413	9.196	9.227	8.009	8.338	7.603	8.473
	1	C	.068	.469	1.133	1.233	1.533	.395	.853
3		S	3.461	3.353	3.663	3.502	3.571	3.132	3.392
	2	C	2.454	2.343	2.043	2.125	1.401	1.633	1.997
3		S	2.223	3.545	1.894	2.130	3.256	1.874	2.358
	3	C	1.620	.514	.975	1.345	-.052	-.678	.704
3		S	-1.586	.861	-.879	-.574	-.350	-1.357	-.610
4	0	C	-6.177	-5.883	-6.054	-4.850	-6.422	-5.971	-5.984
	1	C	-.918	-1.143	-.537	-.270	-1.082	-.248	-.599
4		S	3.825	2.875	3.212	2.523	1.797	1.178	2.637
	2	C	-1.534	-.213	-2.121	-2.538	-2.245	-.540	-1.537
4		S	.143	1.093	1.143	-.024	-.073	.302	.394
	3	C	-1.379	-2.007	-1.923	-.302	.005	-.984	-1.008
4		S	-.145	.370	-.152	-.506	-2.420	.348	-.278
	4	C	-1.069	-1.426	-2.020	-1.912	-2.050	-2.892	-1.992
4		S	.402	-.726	.901	.589	-1.078	.043	.115
5	0	C	-2.866	-1.936	-2.530	-1.667	-1.552	-1.104	-2.053
	1	C	-1.145	-1.456	-2.258	-2.379	-2.772	-1.708	-1.883
5		S	-2.081	-3.241	-2.875	-3.209	-3.015	-1.692	-2.645
	2	C	-1.325	-.725	-1.221	-2.209	-1.963	-2.114	-1.555
5		S	-.332	-.557	-1.583	-.630	-.602	.607	-.506
	3	C	-.074	-.272	.901	-1.128	.554	-.253	-.079
5		S	2.429	1.625	1.289	.638	1.785	2.175	1.695
	4	C	-1.131	-1.077	-1.726	.249	-.233	-2.198	-1.090
5		S	-.075	-1.681	-.341	.153	1.267	-.050	-.209
	5	C	-1.355	-2.068	-1.387	-2.310	-1.540	.952	-1.336
		S	-1.040	.274	-1.412	-1.394	-1.108	-.396	-.886
First day . . . . .			August 2	August 6	August 10	August 14	August 19	August 22	August 2
Last day . . . . .			August 4	August 8	August 12	August 16	August 20	August 24	August 31
Number of measurements . .			8796	6465	8696	7625	5469	6913	45 942
RMS residual . . . . .			9.564	9.108	9.467	9.135	8.987	9.091	10.016

TABLE III.- COEFFICIENTS OF SPHERICAL HARMONIC REPRESENTATION  
AT TOP OF ATMOSPHERE

n	m	Coefficient	Coefficients for duty cycle -						Monthly average
			1	2	3	4	5	6	
0	0	C	235.632	234.822	234.671	235.887	236.723	235.744	235.408
1	0	C	12.347	11.166	12.554	11.847	11.897	10.663	11.827
1	1	C	5.021	5.074	3.600	3.690	3.918	2.447	3.725
		S	-3.795	-2.450	-3.824	-4.430	-2.290	-1.810	-3.267
2	0	C	-22.805	-23.065	-21.476	-24.060	-23.872	-23.838	-23.046
2	1	C	3.196	5.830	5.597	2.927	3.700	3.730	3.982
		S	-1.048	-2.394	-2.528	-1.146	-1.193	-2.177	-1.725
2	2	C	4.036	5.798	5.299	5.295	4.153	5.145	4.985
		S	5.171	3.892	5.509	2.743	3.100	1.753	3.755
3	0	C	12.685	13.866	13.913	12.077	12.572	11.464	12.776
3	1	C	.102	.707	1.708	1.859	2.311	.595	1.286
		S	5.219	5.056	5.524	5.281	5.385	4.723	5.114
3	2	C	3.700	3.533	3.080	3.205	2.113	2.462	3.011
		S	3.352	5.345	2.856	3.212	4.910	2.826	3.556
3	3	C	2.442	.775	1.470	2.028	-.078	-1.022	1.061
		S	-2.391	1.299	-1.326	-.865	-.527	-2.046	-.920
4	0	C	-9.951	-9.476	-9.751	-7.813	-10.344	-9.618	-9.639
4	1	C	-1.479	-1.841	-.865	-.435	-1.743	-.399	-.965
		S	6.161	4.632	5.174	4.065	2.894	1.898	4.248
4	2	C	-2.471	-.342	-3.416	-4.089	-3.616	-.870	-2.477
		S	.231	1.760	1.840	-.039	-.118	.487	.635
4	3	C	-2.221	-3.233	-3.098	-.487	.009	-1.585	-1.623
		S	-.234	.596	-.244	-.815	-3.298	.560	-.442
4	4	C	-1.722	-2.297	-3.253	-3.080	-3.303	-4.659	-3.209
		S	.648	-1.169	1.452	.949	-1.737	.069	.185
5	0	C	-5.005	-3.381	-4.418	-2.911	-2.710	-1.929	-3.585
5	1	C	-2.000	-2.542	-3.944	-4.155	-4.840	-2.984	-3.288
		S	-3.634	-5.661	-5.020	-5.604	-5.265	-2.956	-4.619
5	2	C	-2.314	-1.266	-2.133	-3.858	-3.428	-3.692	-2.716
		S	-.580	-.973	-2.765	-1.099	-1.051	1.060	-.884
5	3	C	-.129	-.475	1.574	-1.970	.968	-.441	-.139
		S	4.242	2.837	2.250	1.114	3.117	3.799	2.960
5	4	C	-1.976	-1.881	-3.015	.434	-.407	-3.839	-1.904
		S	-.131	-2.936	-.595	.267	2.212	-.088	-.365
5	5	C	-2.366	-3.612	-2.423	-4.034	-2.690	1.662	-2.334
		S	-1.816	.478	-2.465	-2.435	-1.936	-.692	-1.547

TABLE IV.- DEGREE DISPERSION

n	$\sigma_n$ for duty cycle -						Monthly average
	1	2	3	4	5	6	
(a) Satellite altitude							
0	173.02	172.43	172.32	173.21	173.83	173.11	172.86
1	10.00	9.03	9.82	9.51	9.19	8.00	9.25
2	16.72	17.37	16.47	17.43	17.25	17.32	16.93
3	9.94	10.73	10.46	9.44	9.86	8.73	9.72
4	7.70	7.22	7.85	6.38	7.87	6.85	7.12
5	5.08	5.32	5.77	5.75	5.67	4.75	4.91
(b) Top of atmosphere							
0	235.63	234.82	234.67	235.89	236.72	235.74	235.41
1	13.86	12.51	13.61	13.18	12.73	11.09	12.82
2	23.97	24.91	23.61	24.99	24.74	24.83	24.27
3	14.99	16.18	15.77	14.24	14.87	13.17	14.65
4	12.40	11.63	12.65	10.28	12.67	11.04	11.47
5	8.88	9.28	10.07	10.04	9.90	8.29	8.53

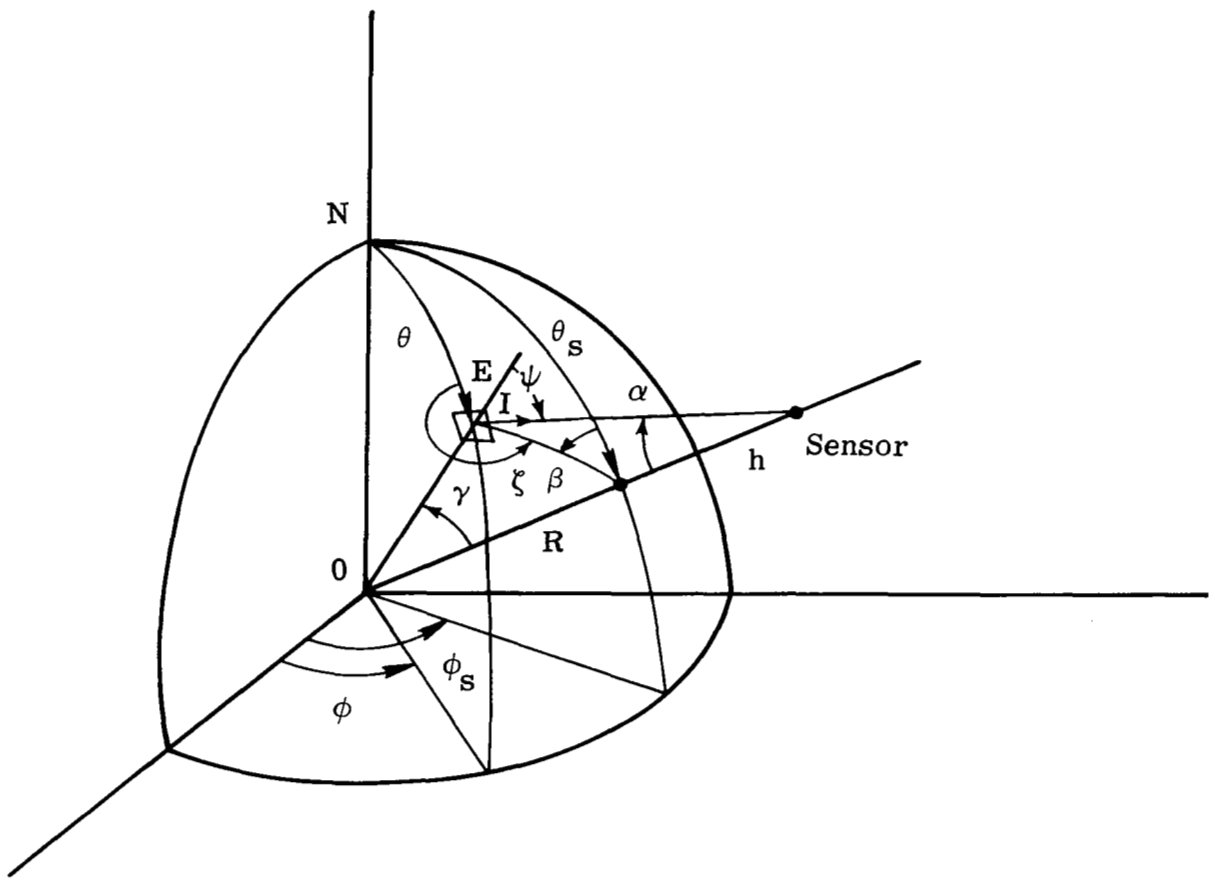


Figure 1.- Earth-satellite geometry.

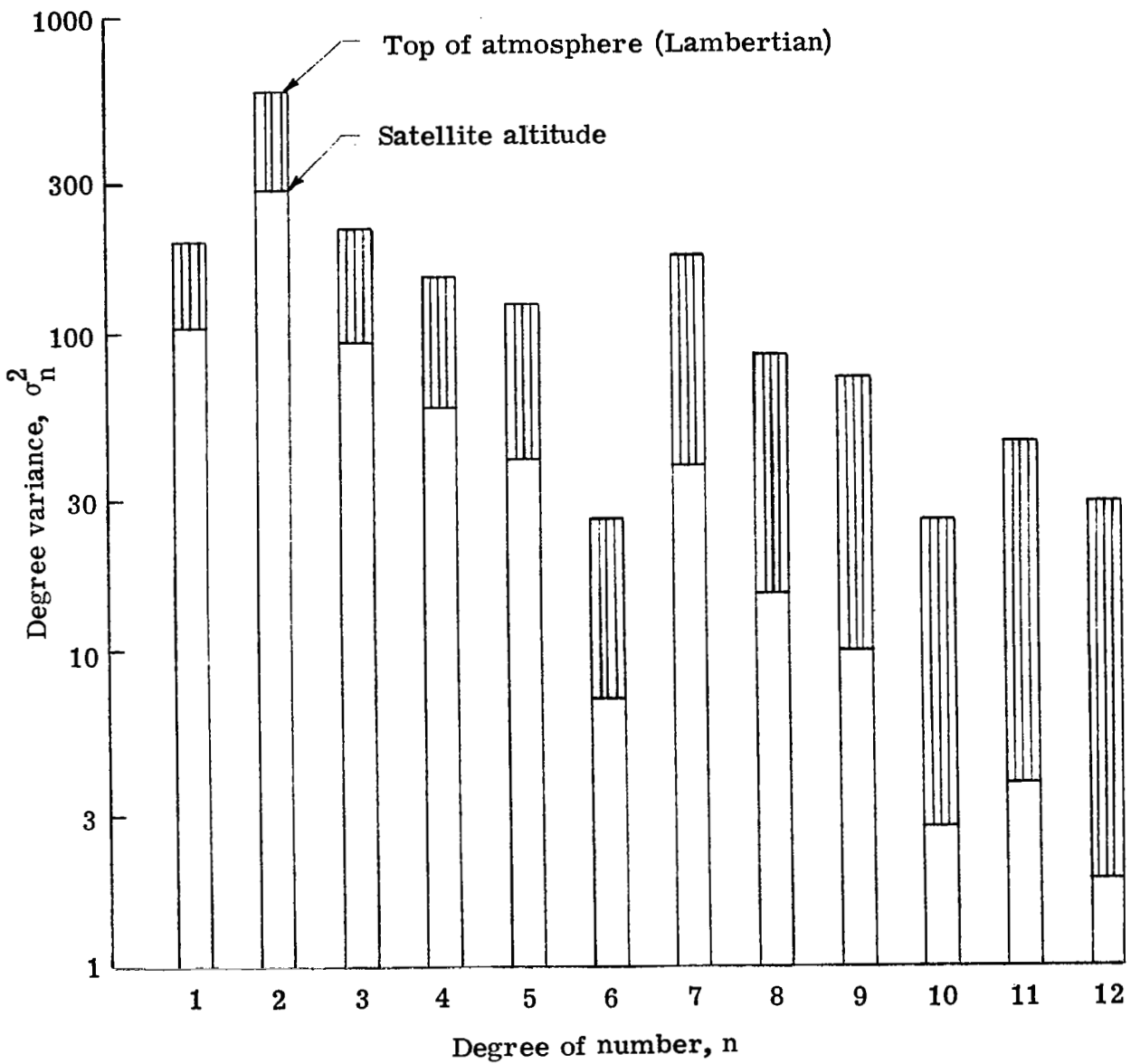


Figure 2.- Degree variance for August 2-4, 1975.

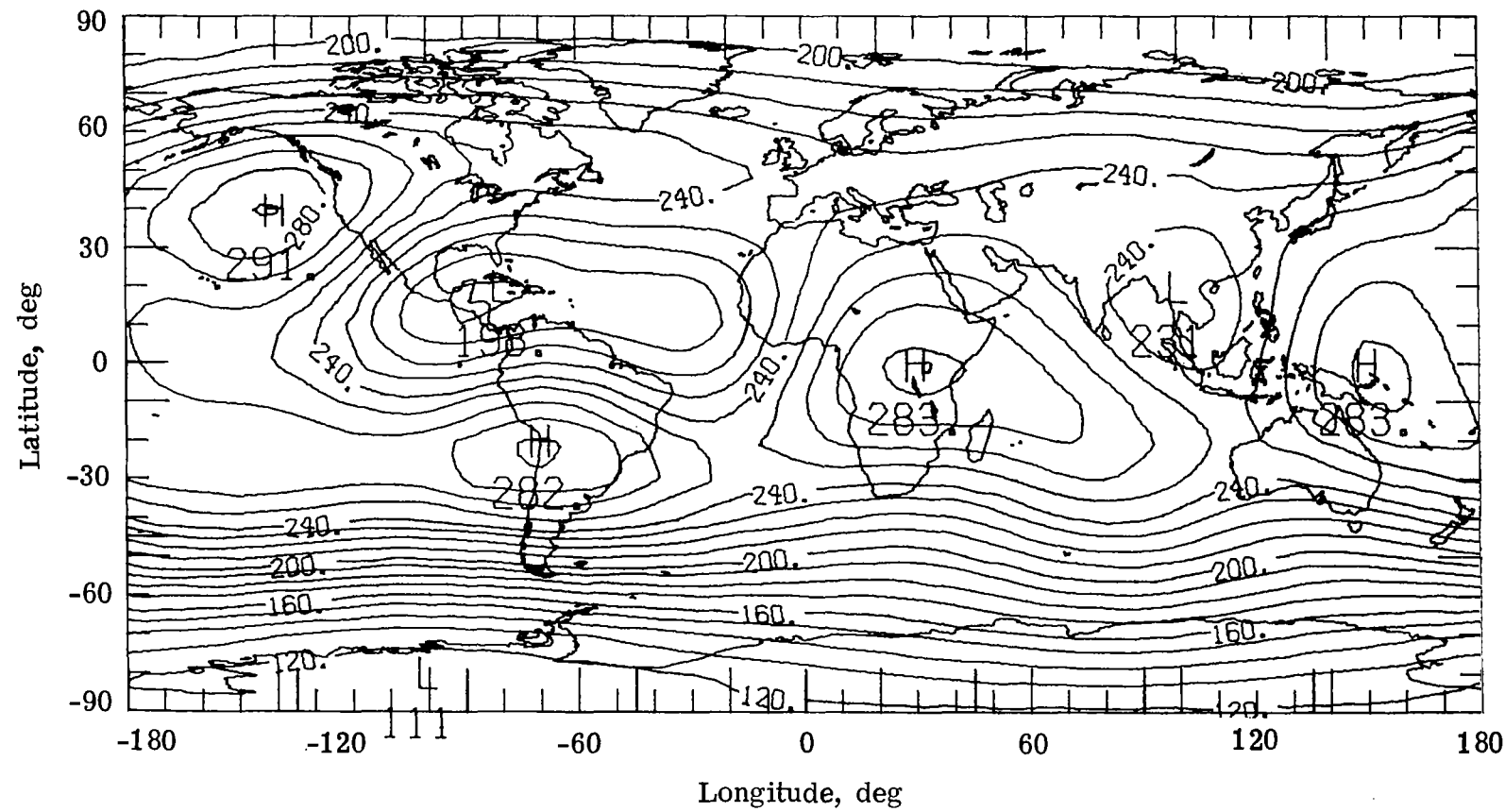


Figure 3.- Map of longwave radiation at top of atmosphere for August 2-4, 1975.

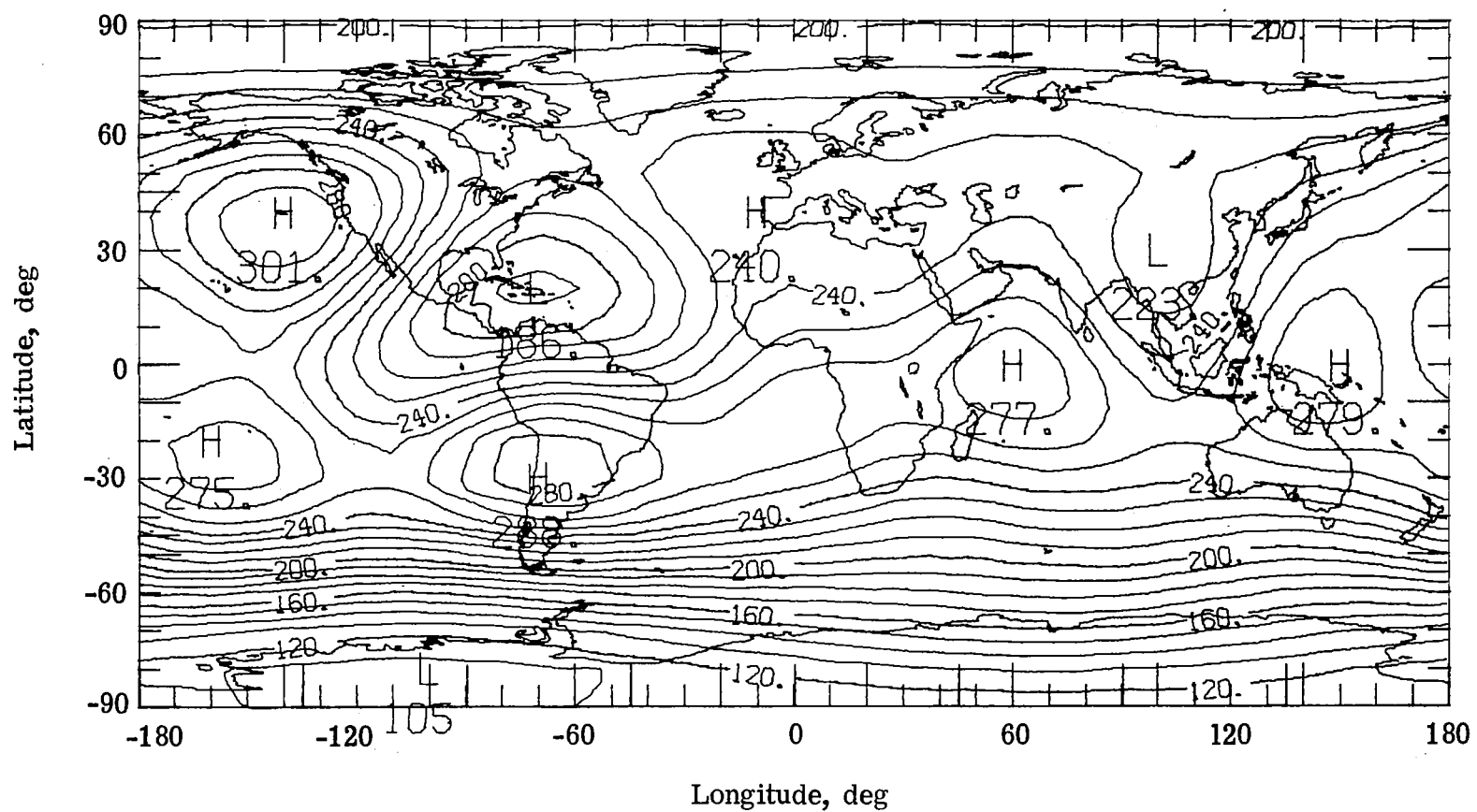


Figure 4.- Map of longwave radiation at top of atmosphere for August 6-8, 1975.

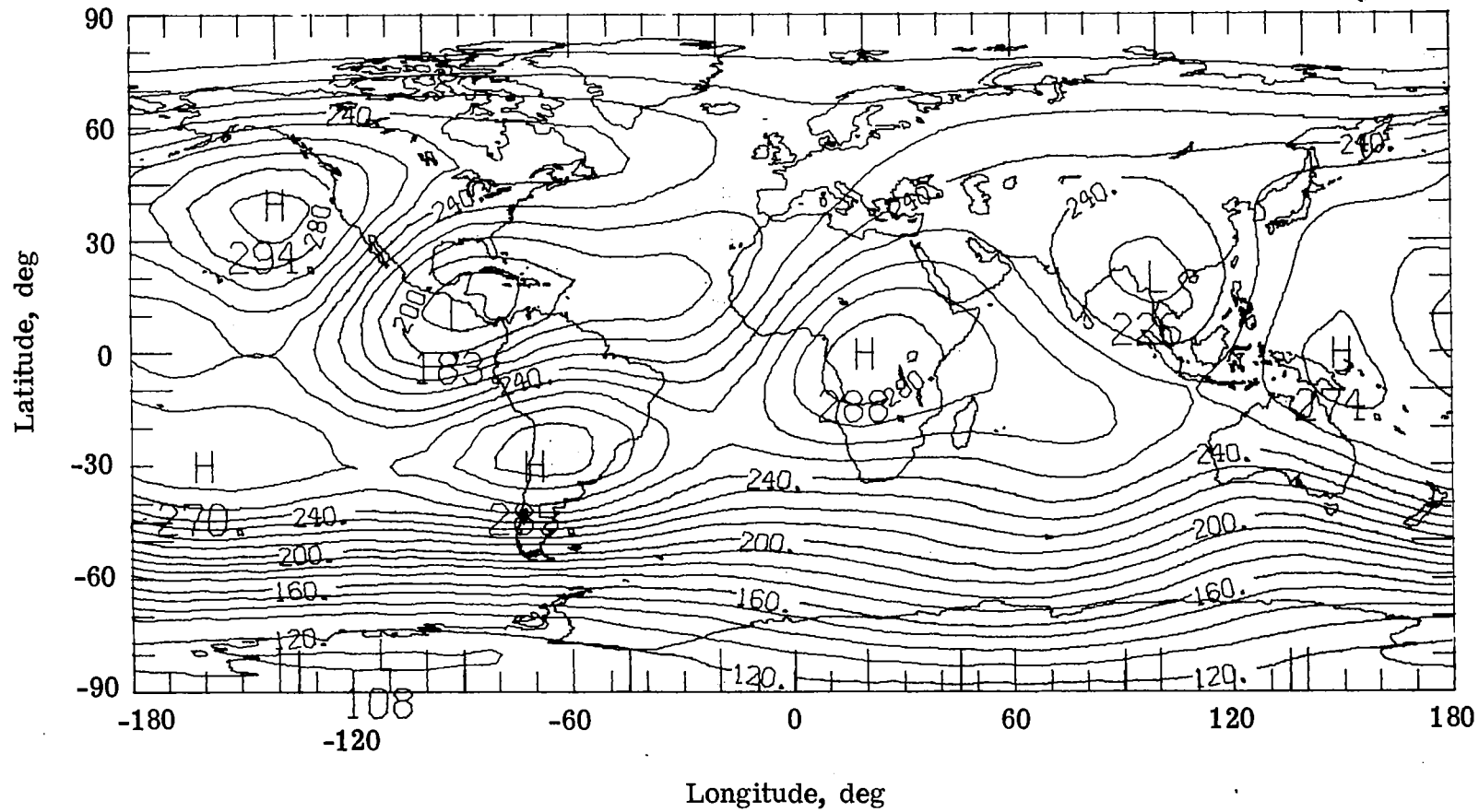


Figure 5.- Map of longwave radiation at top of atmosphere for August 10-12, 1975.

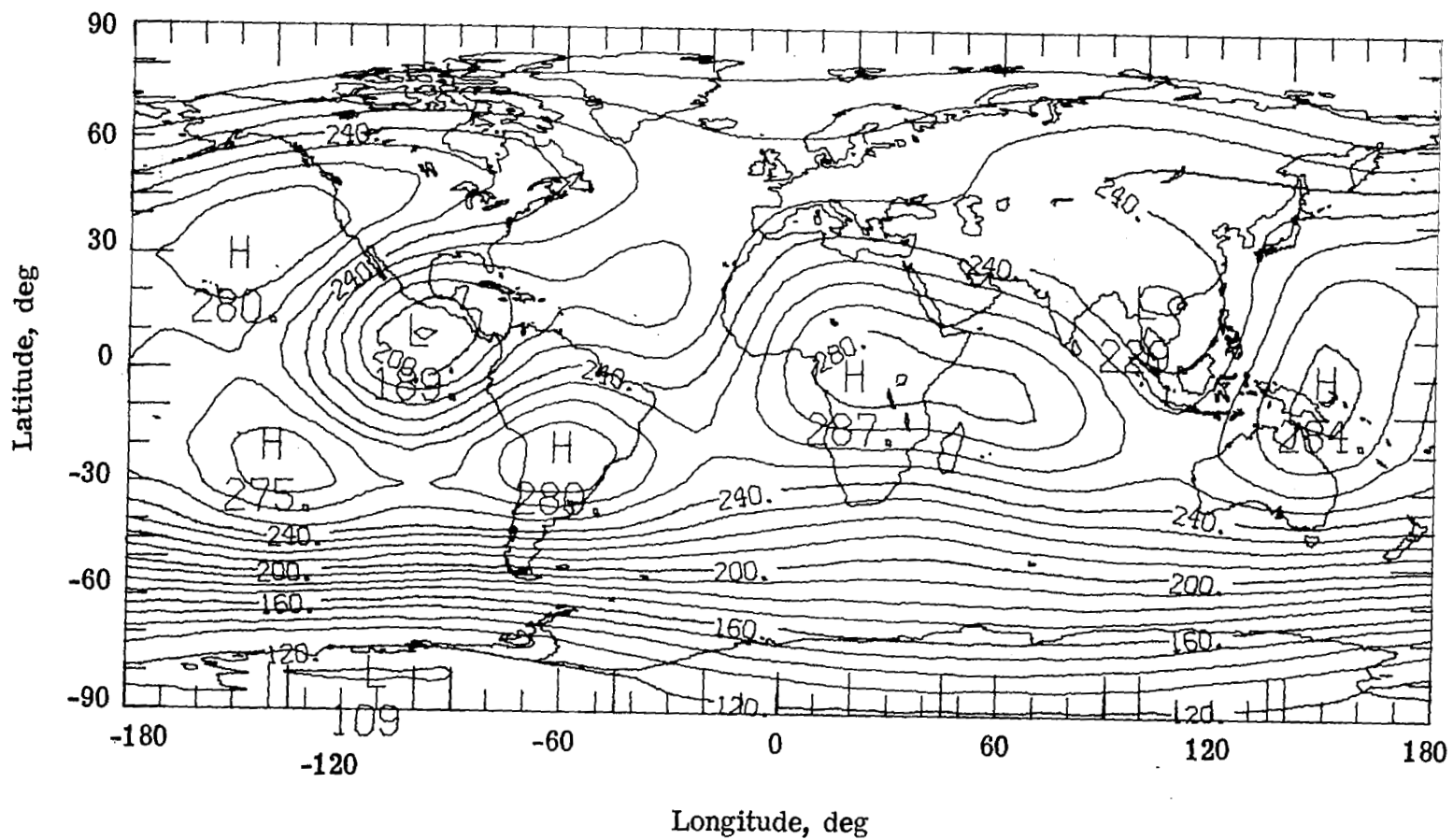


Figure 6.- Map of longwave radiation at top of atmosphere for August 14-16, 1975.

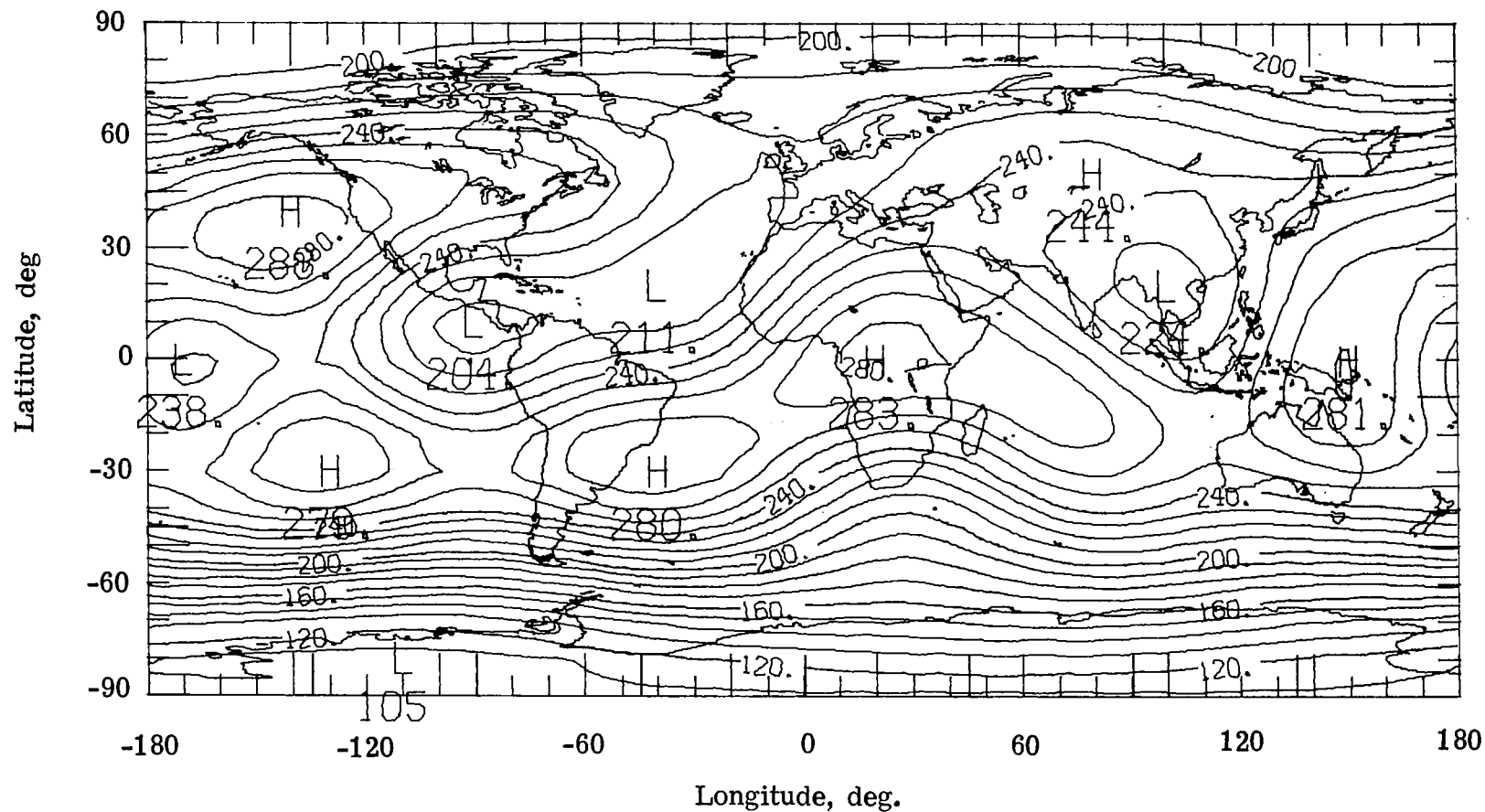


Figure 7.- Map of longwave radiation at top of atmosphere for August 19-20, 1975.

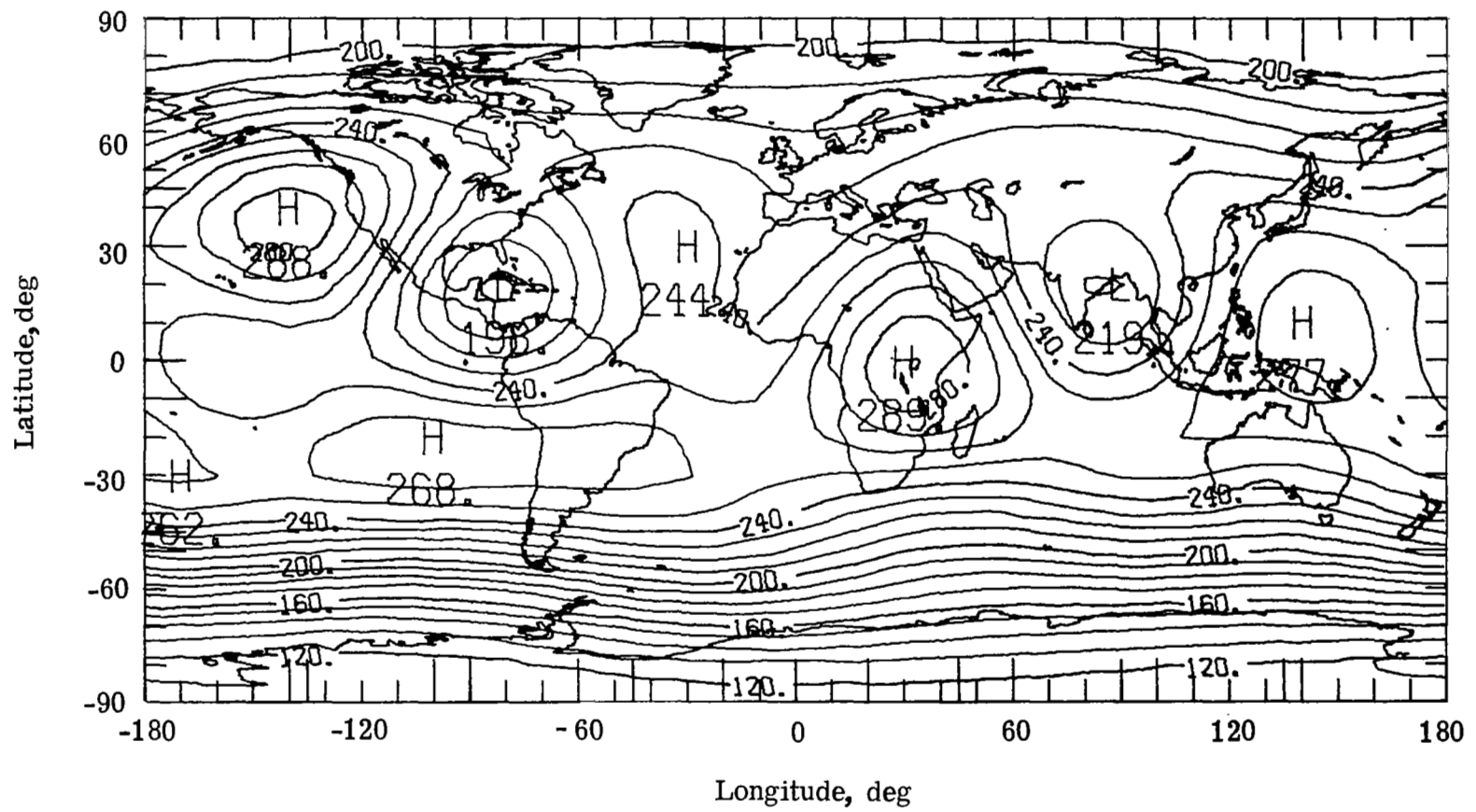


Figure 8.- Map of longwave radiation at top of atmosphere for August 22-24, 1975.

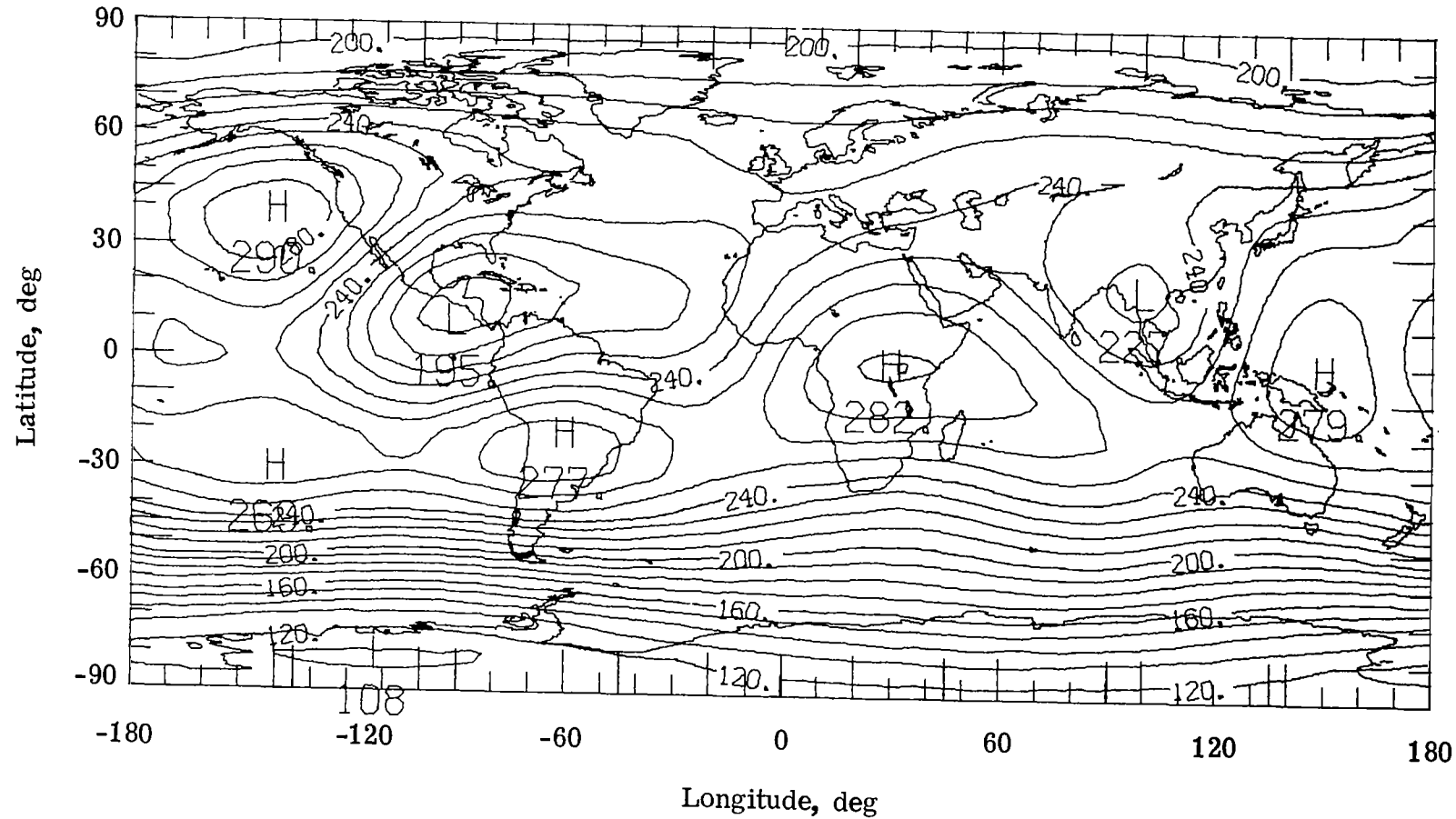


Figure 9.- Map of average longwave radiation at top of atmosphere for August 1975.

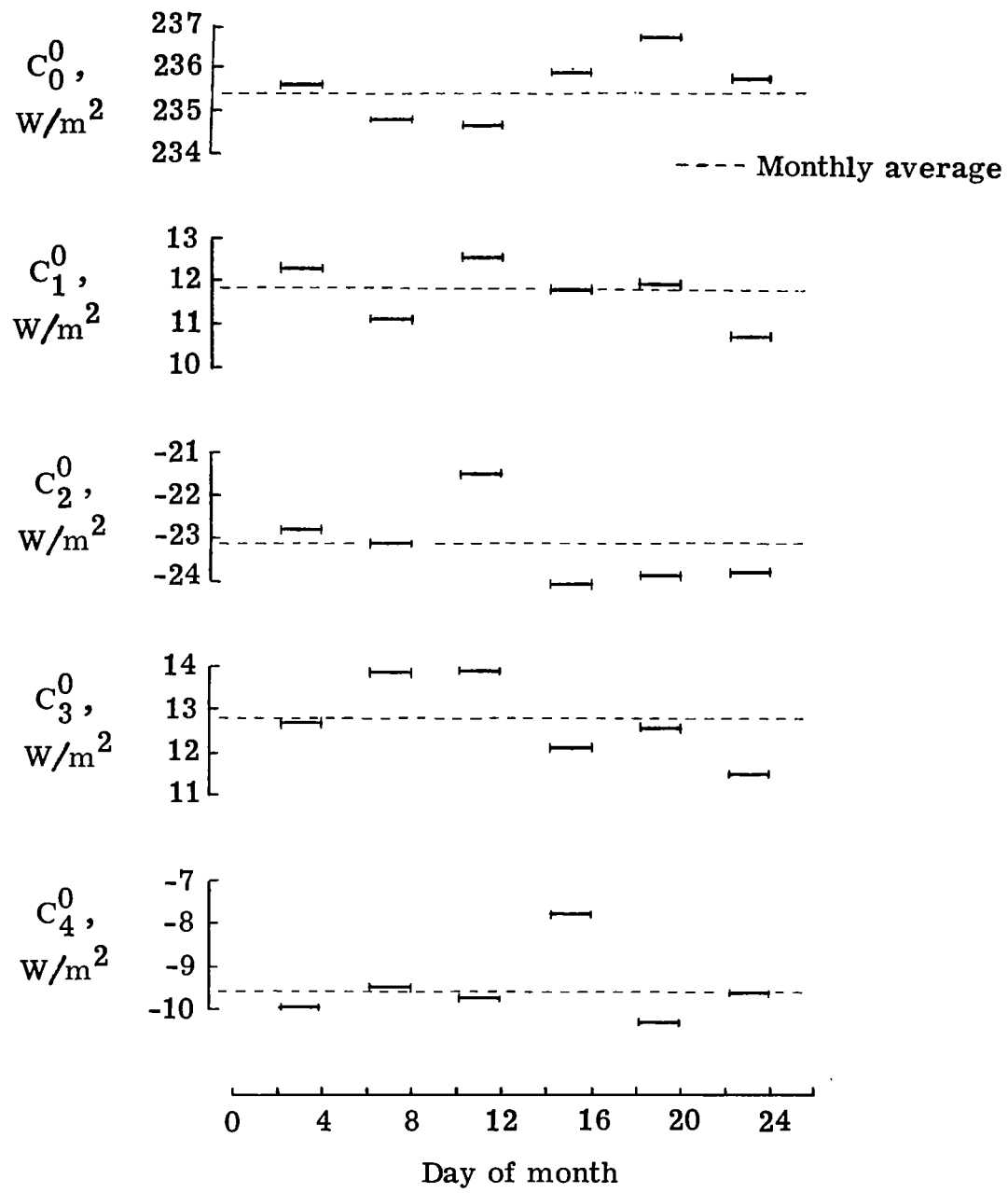


Figure 10.- Time variation of zonal coefficients for longwave radiation at top of atmosphere for August 1975.

1. Report No. NASA TP-1307	2. Government Accession No.	3. Recipient's Catalog No.	
4. Title and Subtitle  PARAMETER ESTIMATION APPLIED TO NIMBUS 6 WIDE-ANGLE LONGWAVE RADIATION MEASUREMENTS		5. Report Date December 1978	
		6. Performing Organization Code	
7. Author(s) Richard N. Green and G. Louis Smith		8. Performing Organization Report No. L-12233	
9. Performing Organization Name and Address  NASA Langley Research Center Hampton VA 23665		10. Work Unit No. 175-40-30-02	
12. Sponsoring Agency Name and Address  National Aeronautics and Space Administration Washington, DC 20546		11. Contract or Grant No.	
15. Supplementary Notes		13. Type of Report and Period Covered Technical Paper	
		14. Sponsoring Agency Code	
16. Abstract  A parameter estimation technique has been used to analyze the August 1975 Nimbus 6 Earth radiation budget (ERB) data to demonstrate the concept of deconvolution. The longwave radiation field at the top of the atmosphere is defined from satellite data by a fifth degree and fifth order spherical harmonic representation. The variations of the major features of the radiation field are defined by analyzing the data separately for each two-day duty cycle. A table of coefficient values for each spherical harmonic representation is given along with global mean, gradients, degree variances, and contour plots. In addition, the entire data set is analyzed to define the monthly average radiation field.			
17. Key Words (Suggested by Author(s))  Longwave radiation Nimbus 6 Earth radiation budget data Parameter estimation Deconvolution Spherical harmonics		18. Distribution Statement  Unclassified - Unlimited  Subject Category 47	
19. Security Classif. (of this report) Unclassified	20. Security Classif. (of this page) Unclassified	21. No. of Pages 37	22. Price* \$4.50

\* For sale by the National Technical Information Service, Springfield, Virginia 22161

NASA-Langley, 1978

National Aeronautics and  
Space Administration

Washington, D.C.  
20546

Official Business

Penalty for Private Use, \$300

THIRD-CLASS BULK RATE

Postage and Fees Paid  
National Aeronautics and  
Space Administration  
NASA-451



1 110, E. 111378 S00903DS  
DEPT OF THE AIR FORCE  
AF WEAPONS LABORATORY  
ATTN: TECHNICAL LIBRARY (SUL)  
KIRTLAND AFB NM 87117

NASA

POSTMASTER:

If Undeliverable (Section 158  
Postal Manual) Do Not Return